Stay on the leading edge of stem cell research

The Gibco™ 5 Days of Stem Cells virtual event connects you to the latest stem cell techniques, research breakthroughs, and esteemed scientists from around the world–all from the comfort of anywhere

We'll share developments, discoveries, and cutting-edge content connected to a wide variety of stem cell applications, including disease modeling, cell and gene therapy, 3D modeling, and much more.

The 5-day virtual agenda is packed full of incredible insights in the form of:

- Leading scientific presentations from thought leaders around the world
- Behind-the-scenes virtual training demos
- Scientific poster sessions
- Hundreds of key stem cell tools and resources
- A global network of researchers including our stem cell experts and technical support

It's all happening October 12–16, 2020.

CURRENT PROTOCOLS
A Wiley Brand

Register for free at **thermofisher.com/5daysofstemcells**

ThermoFisher
SCIENTIFIC

Ana Valinhas ORCID iD: 0000-0002-4683-1577

Microcarrier expansion of c-MycER^{TAM} - modified human olfactory mucosa cells for neural regeneration

Author 1: Ana Valinhas[1]
Author 2: Gerardo Santiago-Toledo[1],
Corresponding author: Ivan B. Wall [1,2,3]
[1] Department of Biochemical Engineering, University College London, London WC1E 6BT, UK
[2] Aston Medical research Institute and School of Life and Health Sciences, Aston University, Birmingham, B4 7ET, UK
[3] Institute of Tissue Regeneration Engineering (ITREN), Dankook University, Cheonan, 31116, Republic of Korea
Contact details
Author 1: ana.valinhas.14@ucl.ac.uk, +44 7399410283
Author 2: gerardo.santiago.14@ucl.ac.uk, +44 7958513507
Corresponding author: i.wall@aston.ac.uk, +44 7886 652111

Abstract

Human olfactory mucosa cells (hOMCs) have potential as a regenerative therapy for spinal cord injury. In our earlier work we derived PA5 cells, a polyclonal population that retains functional attributes of primary human OMCs. Microcarrier suspension culture is an alternative to planar 2D culture to produce cells in quantities that can meet the needs of clinical development. This study aimed to screen the effects of 10 microcarriers on PA5 hOMCs yield and phenotype. Studies performed in well plates led to a 2.9-fold higher cell yield on Plastic compared to Plastic Plus microcarriers with upregulation of neural markers β-III tubulin and nestin for both conditions. Microcarrier suspension culture resulted in concentrations of $1.4x10^5$ cells/mL and $4.9x10^4$ cells/mL for Plastic and Plastic Plus, respectively, after 7 days. $p75^{NTR}$ transcript was significantly upregulated for PA5 hOMCs grown on Plastic Plus compared to Plastic. Furthermore, co-culture of PA5 hOMCs grown on Plastic Plus with a neuronal cell line (NG108-15) led to increased neurite outgrowth. This study shows successful expansion of PA5 cells using suspension culture on microcarriers, and it reveals competing effects of microcarriers on cell expansion versus functional attributes, showing that designing scalable bioprocesses should not only be driven by cell yields.

Key words: human olfactory mucosa cells, spinal cord injury, allogeneic cell therapy, microcarrier, suspension culture

Introduction

250,000 to 500,000 people are affected by spinal cord injury every year worldwide (Bickenbach et al., 2013). The spinal cord is part of the central nervous system (CNS), and unlike the peripheral nervous

system (PNS), has limited regenerative capacity after injury (Ahuja et al., 2017). The slow regenerative capacity of the CNS is attributed to the generation of a "glial scar" after injury which constitutes a barrier for axonal regrowth. Human olfactory mucosa cells (hOMCs) have shown promising results in both pre-clinical and clinical studies for the treatment of spinal cord injury (SCI) (F. Féron et al., 2005; Iwatsuki et al., 2008; Mackay-Sim et al., 2008; Tabakow et al., 2013). The regenerative capacity of OMCs is attributed to their unique ability to support the regeneration of olfactory receptor neurons (ORNs) which extended their axons from the PNS to the CNS, a property unique to the olfactory system in mammals (R. Doucette, 1991). The hOMC population can be obtained through biopsies of the olfactory mucosa, a source safer than the olfactory bulb which requires invasive intracranial surgery to be accessible (François Féron et al., 1998; Jani & Raisman, 2004). After biopsy, the cell population is subjected to a differential adhesion step to enrich neuroprotective cell types such as OECs, late adherent primary hOMCs, by removing rapidly adherent cells (i.e. fibroblasts) considered to be contaminants (Santiago-Toledo et al., 2019, Nash et al 2001). Early and recent studies have attributed the neural regeneration of the hOMC population to the presence of several different cell types, such as neural stem cells (NSCs), mesenchymal stem cells (MSCs), olfactory neurons and olfactory ensheathing cells (OECs), a type of glia (Delorme et al., 2010; J. R. Doucette, 1984; Lindsay et al., 2013; Wolozin et al., 1992). Markers reported in hOMCs primary populations include glial ($p75^{NTR}$, GFAP and S100β), neural stem cell (nestin), early neural differentiation (β-III tubulin), mesenchymal, and fibroblast associated markers (CD90/Thy1 and fibronectin) (Au et al., 2002; Bianco et al., 2004; Hahn et al., 2005; Kawaja et al., 2009).

Reported clinical trials have used an autologous approach which can lead to variable outcomes. Since hOMCs populations are highly variable between patients, these are challenging to expand and there is a lack of consistency between protocols used for tissue biopsy and preparation of cells for transplant (F Féron et al., 1999). Therefore, it would be beneficial to develop an allogeneic or universal "off-the-shelf" approach. We previously reported the generation of a candidate cell line from late-adherent hOMCs by genetic modification of primary cells with c-$MycER^{TAM}$ conditional immortalization technology, to advance a potential allogeneic therapeutic product for the treatment of SCI denominated PA5 hOMCs (Santiago-Toledo et al., 2019). It is yet unclear whether a unique cell type within a hOMCs population is responsible for neural regeneration, or whether there is benefit in transplanting several types of cells within the population (Anna et al., 2017; Reshamwala et al., 2019). Clones from polyclonal populations such as PA5 hOMCs can be further derived, expanded, banked and screened to generate an allogeneic cell therapy product for the treatment of SCI. The generation of a conditionally-immortalized hOMC population, such as PA5 hOMCs, enables a potentially extended life span, allowing the application of a cell-banking model-based manufacturing process, necessary for an allogeneic cell therapy.

The translation of such a therapeutic product to the market would require the development of a scalable bioprocess, able to yield large amounts of cells which can reach doses up to $1x10^7$ cells/dose (Casarosa et al., 2014). Commonly, adherent or anchorage-dependent cells have been grown in two-dimensional platforms such as tissue-culture flasks, cell factories and automated systems. Even though these systems are reliable due to their wide spread use in the industry, they are not easily scalable for

producing large quantities of allogeneic cells, making them unsuitable for commercial stages (Brandenberger et al., 2011; Simaria et al., 2014). Among available technologies, microcarriers are a suitable alternative to perform expansion of adherent cells in a scalable manner in stirred tank bioreactors and offer a higher larger surface per unit volume of bioreactor. It may be feasible to manufacture early-stage clinical products using planar systems and then transition to stirred tank bioreactors for late-stage clinical trials and commercialisation, yet this would require significant validation work to meet regulatory approval, and risk product specification failure later in development due to manufacturing process changes. Therefore, early adoption of market scale manufacturing technology is necessary.

Microcarrier cell culture platforms have been reported for the successful expansion of mesenchymal stem cells (MSCs) (dos Santos et al., 2014; Rafiq et al., 2013), embryonic stem cells (ESCs) (Oh et al., 2009) and induced pluripotent stem cells (iPSCs) (Badenes et al., 2017; Carlos AV Rodrigues et al., 2018). Stirred tank bioreactors are well explored systems that enable the monitoring and control of several culture parameters such as oxygen tension, pH and agitation regimes. These platforms also offer a closed bioprocess environment with reduced operator interference and variability. Therefore, these are platforms that offer more robust and reproducible bioprocesses that theoretically can deliver consistent quality products, compliant with Good Manufacturing Practice (GMP) and Good Clinical Practice (GCP) requirements.

In this work, we report the microcarrier expansion of a candidate cell population for the treatment of SCI, PA5 hOMCs, on microcarrier stirred culture using spinner flasks, with the aim to identify a microcarrier type that maximize the expansion of neuroprotective cell types such as OECs, NSCs, and MSCs, which can lead to increased potency. First, a variety of commercially available microcarriers were selected based on a screening methodology using ultra-low attachment 96-well plates. Besides the suitability of the microcarrier, considerations of compliance for good manufacturing practices (GMP) and adaptability to xeno-free conditions were considered for microcarriers selection. Then, cells were grown on two types of microcarriers using spinner flasks, based on protocols previously reported for the expansion of hMSCs (Santos et al., 2011). To further understand growth kinetics, PA5 hOMCs were grown on microcarriers for 7 days. Cell phenotype was assessed through immunocytochemistry and RT-qPCR. Potency of PA5 hOMCs was assessed through the capacity of the harvested cells to promote neurite outgrowth using a co-culture assay of hOMCs and NG108-15 neurons.

We report the use of a microcarrier-based spinner flasks system for the expansion of the PA5 hOMCs population of cells, a candidate cell line for the treatment of spinal cord-injury.

Materials and methods

hOMC monolayer culture

PA5 hOMCs were expanded in T-flasks, freshly coated with poly-L-lysine (PLL, Sigma, UK, 100 µg/mL), using as complete medium DMEM/F12 + Glutamax^{TM} (Gibco, Life Technologies, UK) supplemented with 10% fetal bovine serum (FBS) (Sigma, Germany) and 4-hydroxitamoxifen (4-OHT', 1:10,000). Cells were maintained in a standard incubator (37□C, 5% CO_2 in air). A seeding density of 6000 cells/cm^2 was used and feeding was performed every two days. Cells were passaged when 60-80% confluency was reached, through incubation with TryPLE (Gibco, UK) for 5 minutes.

The dissociation reagent was quenched with complete medium and the cell suspension was centrifuges for 5 minutes at 400 x g.

Microcarrier screening in well plates

10 commercially available microcarriers were tested for expansion of PA5 hOMCs in ultra-low attachment 96-well plates: Plastic, Plastic Laminin Coated (Plastic L), Plastic Plus, PronectinF®, Collagen, FACT III, Star-Plus, Hillex II, all from Pall, UK. Synthemax II ® (Low and High Concentration) (Corning, UK) and Cytodex I (GE Healthcare, UK) were also used. Microcarriers specifications are shown on Table 1. Sterilization of Pall microcarriers and Cytodex I microcarriers was achieved by resuspension in distilled water (Gibco, UK) and PBS Ca+ and Mg+ free (Lonza, UK), respectively, followed by autoclaving at 121 ºC for 15 min. Synthemax II ® microcarriers were sterilized under a UV lamp for 90 minutes.

A monolayer of microcarriers with a total surface area of 1.28 cm^2 was used per well, in order to cover the bottom of a 96-well plate well. For 6-well plates, a monolayer of microcarriers with a total surface area of 38 cm^2 was used per well. Total working volumes were of 200 µL and 6 mL for 96-well plates and 6-well plates, respectively. Plastic L microcarriers were incubated with a solution of 20 µg/mL Cultrex ® Mouse Laminin I (Trevigen, UK) for 1 hour in a standard incubator prior to cell seeding. All microcarriers were let to equilibrate for 1 hour in a standard incubator with complete medium. A seeding density of 6000 cells/cm^2 was used. Medium exchanges were performed for 50% of the total volume, every two days. Cells were culture in ultra-low 96-well plates for a total of 7 days. For 96 well-plates, relative viable cell number was measured using the cell Counting Kit-8 (CCK-8) (Dojindo, Japan) every time medium exchanges were performed. Briefly, 10 µL of reagent were added per 100 µL of microcarrier suspension. After incubation for 1 hour in a standard incubator, the supernatant was transferred to a 96-well plate and absorbance readings at 450 nm were performed in a microplate reader (Tecan, Switzerland). Quantification of the of cells per well was performed based on a standard curve performed on the first day of culture.

Spinner-flask culture

The protocol used for spinner flask culture was based on Santos et al 2011. Suspension culture experiments were performed in 100-mL flat bottom spinner-flasks (Bellco) with 80 mL as working volume. Spinner-flasks were siliconized using Sigmacote (Sigma, Germany) to avoid cell attachment. After applying the reagent to all the glass surface and aspirating it, vessels were let to dry for 24 hours in a fume hood. After, vessels were rinsed three times with distilled water (Gibco, UK). Plastic and Plastic Plus microcarriers were used for spinner-flask culture with a total surface area of 518.4 cm^2. Microcarriers were prepared by autoclaving in distilled water (Gibco, UK) for 121 ºC for 15 min. After, the distilled water was aspirated as much as possible and complete medium was added. Microcarriers were let to equilibrate for 1 hour in a standard incubator. 60-80% confluent PA5 hOMCs were detached as described in section “hOMC cell culture” and an adequate amount of cells was added to the tube containing the microcarriers suspension in complete medium to a seeding density of 6000 cells/cm^2. After transferring the microcarrier and cell suspension to spinner-flasks containing adequate amounts of complete medium, an agitation of 40 rpm was started. Spinner-flasks were maintained on a Bell-Ennium™ Compact 5 position magnetic stirrer platform (BellCo) in a standard incubator. In order to allow for air exchange, a side-arm of the spinner-flask was kept loosened (half a turn of the cap).

Cell expansion was maintained for 7 days. Feeding was performed every two days by removing 50% of the expanded medium and adding the same amount of fresh complete medium. Sampling, also performed every two days, was achieved by retrieving 2 mL of a homogeneous microcarriers suspension for manual cell counting and immunocytochemistry. Cell counting and viability measurements were performed by trypan blue exclusion, using a haemocytometer.

Harvest

Exhausted medium was retrieved from the vessel and the microcarrier-cell suspension was washed with 40 mL of HBSS (Gibco, UK) twice. 20 mL of TryPLE Select (Gibco, UK) were incubated with the microcarrier-cell suspension for 15 minutes, at an agitation of 100 rpm in a standard incubator. To quench the dissociation reagent, 30 mL of complete medium were added. The suspension was passed through 40 µm cell strainers and centrifuged for 5 minutes at 400 xg. Harvested cells were counted using the trypan blue exclusion method and were either pelleted for RT-qPCR or plated at 6000 cells/cm^2 to perform several assays such as immunocytochemistry and NG108-15 co-culture assay.

Analytical techniques

Metabolite analysis

On the days medium exchange occurred, metabolite analysis was performed using the the CuBian HT270 analyzer (Optocell GmbH & Co, KG, Germany to obtain the concentration of glucose, lactate and ammonia.

Immunocytochemistry

Samples were fixed using a solution of 4% PFA in PBS for 20 minutes at RT. After washing with PBS (Lonza) for 5 minutes, twice, permeabilization was done through incubation of samples with a solution of 0.1% Triton X-100 (Sigma) in PBS for 20 minutes at room temperature. After washing samples twice with PBS for 5 minutes, samples were incubated with a blocking solution of 5% Goat Serum (DAKO) in PBS for 1 hour at room temperature. Primary antibodies against p75^{NTR} (Millipore), fibronectin (Sigma), CD90 (Millipore), nestin (Millipore), GFAP (Dako), S100β (Dako) and β-III tubulin (Sigma) (Table 2) were used with a dilution of 1:200 in blocking solution and incubated for 90 minutes at room temperature. After washing with PBS, secondary antibodies (Goat anti-rb IgG (H+L)-Alexa Fluor 594; Goat anti-Ms (H+L)-Alexa Fluor 488, Invitrogen) and Hoechst 33342 (Molecular Probes) were diluted in blocking solution using a dilution of 1:200 and 1:1000, respectively. Images of planar culture were acquired using the microscope system EVOS® FL (ThermoFisher Scientific), while microcarrier culture 16-bit multi-color montage images were obtained with a Zeiss LSM 880 with Airscan confocal microscope system (Carl Zeiss) and Zen 2009 acquisition software (Carl Zeiss).

qRT-PCR

Cells expanded on microcarriers in ultra-low attachment 6-well plates were detached as previously described. Cell suspensions were centrifuged and excess medium was removed prior to storage at -80^{o}C until further analysis. Pellets were first re-suspended in RLT Buffer (QIAGEN) before being homogenised in Qiashredder Columns (QIAGEN) according to the manufacturer's instructions. Synthesis of complementary deoxyribonucleic acid (cDNA) and removal of genomic DNA was performed using the QIAGEN RT-PCR kit following the manufacturer's instructions. Genomic DNA was eliminated using gDNA Wipeout Buffer (QIAGEN) with up to 1 µg template RNA and RNAse free water in a total reaction volume of 14 µL. The entire 14 µL reaction volume was subsequently

mixed with a MasterMix (Bio-Rad): template RNAs or no template for NTC (no template control), RT Primer Mix Quantiscript RT Buffer and Quantiscript Reverse Transcriptase or with RNA free water for no-RT (No reverse transcriptase control), in a total volume of 20 µL. The qPCR reactions were performed in Bio-Rad Hard-Shell Low Profile Thin-Wall 96 Well Skirted PCR plates on the Bio-Rad CFX 96 Connect Real-Time PCR System using the Quantitect SYBR Green PCR Kits (QIAGEN) according to the manufacturer's instructions. For each reaction Quantitect Mastermix Buffer, Quantitect pre-validated primer assay (Table 2), water and cDNA were combined to make final reaction volumes of 25 µL. On each 96-well plate samples were analysed in triplicate with β-actin as an internal reference control and standard controls No-RT and NTCs to check for cross contamination. The 2-ΔΔCt method was used to analyse the data.

Co-culture assay

A co-culture of NG108-15 neurons with PA5 cells after expansion on microcarriers was used to assess neuron outgrowth. NG108-15 cells (ATCC HB-12317) are a hybrid rodent glioma-neuroblastoma cell line. As a positive control, a rat SCL 4.1/F7 (ECACC 93031294) Schwann cell line was used.

NG108-15 and F7 cells were grown for two passages on T-flasks coated with poly-L-lysine (PLL, Sigma, 100 µg/mL) or uncoated, respectively. When 60-80% confluency was reached, NG108-15 cells were passaged by hitting the flask and re-plated at 6000 cells/cm^2, while F7 cells were passaged following the same protocol used for PA5 hOMCs and re-plated at 6000 cells/cm^2. For the co-culture assay PA5 hOMCs were plated at 6000 cells/cm^2 onto freshly coated 24-well plates with poly-L-lysine (PLL, Sigma, 100 µg/mL). After 24 hours, NG108-15 cells were plated on wells with PA5 hOMCs or F7 cells using a seeding density of 500 cells/well. Medium changes were performed every two days and samples fixed after 5 days. 4-OHT was not added in the medium for this assay. Immunocytochemistry was performed as previously described. Images were acquired with EVOS FL Imaging System (Thermo-Scientific) at a 100x total magnification. 15 frames were acquired per condition (5 per technical repeat) and neurite quantification was performed manually using the NeuronJ (Meijering et al., 2004) plugin in ImageJ.

Statistical methods

The Kolmogorov-Smirnov test was used for data normality and Levene's test was used for homogeneity of variance. For pairwise-comparisons, one-way ANOVA was used with post-hoc Tukey's or Games-Howell test. A difference of $p<0.05$ was considered significant. All tests were performed using OriginPro 2016 (OriginLab, USA).

Formulae

The specific growth rate, µ (day^{-1}):

$$\ln(X) = \mu t + \ln(X_0)$$

Where X is the concentration of cells, X_0 is the concentration of cells at t_0. μ for the exponential phase, considered to be from day 3 to 7.

Doubling time, t_d (days):

$$t_d = \frac{\ln(2)}{\mu}$$

Fold-increase:

$$Fold\ increase = \frac{X_t}{X_0}$$

Where $C_{X(t)}$ is the cell concentration at the end of the culture and $C_{X(0)}$ is the initial cell concentration.

Specific nutrient consumption and metabolite production rate, q_{met} (pmol.cell^{-1}.day^{-1})

$$q_{met} = \frac{\mu}{X_0} \frac{C_{met(t)} - C_{met(0)}}{e^{\mu t} - 1}$$

Where $C_{met(t)}$ and $C_{met(0)}$ are the concentration of metabolite at the end and start of the exponential phase.

Lactate yield from glucose, $Y_{Lac/Glc}$

$$Y_{Lac/Glc} = \frac{\Delta[Lac]}{\Delta[Glc]}$$

Where $\Delta[Lac]$ is the lactate production and $\Delta[Glc]$ is the glucose consumption during the exponential phase.

Results

PA5 hOMCs planner cell culture

PA5 hOMCs were cultured on a monolayer at a seeding density of 6,000 cells/cm^2 for 7 days in 96-well plates. Viable cell counts, performed with the CCK-8 viability reagent, showed increased growth over time, with the highest number of viable cells of 5.5×10^4 reached by day 7 (Figure 1 A). Morphologically, PA5 hOMCs showed an elongated, fibroblastic like shape (Figure 1 B). Cells stained positive for the glial markers p75^{NTR}, S100β, and GFAP which are commonly used to characterise the OEC phenotype (Au et al., 2002; Bianco et al., 2004; Hahn et al., 2005; Kawaja et al., 2009). PA5 hOMCs stained positive for other markers, such as nestin and β-III tubulin, associated with the neuronal phenotype (Gómez-Virgilio et al., 2018; Murrell et al., 2005). The population also stained positive for fibronectin (fibroblast marker) (Ito et al., 2006; Yiu & He, 2006) and CD90 (MSC marker) (C. Chen et al., 2014; Holbrook et al., 2011).

Microcarrier screening for PA5 hOMCs growth on well plates

The growth of PA5 hOMCs was tested on 10 commercially available microcarriers in ultra-low attachment 96-well plates. The growth of PA5 hOMCs was followed over 7 days as this is the length of time for the duration of one passage (Figure 2 A). After seeding on day 0, viable cell number was measured every two days, when media was exchanged. On day 1, viable cell numbers ranged from $8.1\text{x}10^3$ cells/well to $9.6\text{x}10^3$ cells/well for Plastic LC, Synthemax II LC, Synthemax II HC, Plastic, Plastic Plus and FACT II (Figure 2 B). At the same time point, Star-Plus and Cytodex I microcarriers provided a viable cell number between $3.3\text{x}10^3$ to $5.0\text{x}10^3$ cells/well. As shown in Figure 2 C, by day 7, three distinct groups of microcarriers were observed. Plastic and Collagen microcarriers supported high growth of $8.8\text{x}10^4$ and $7.5\text{x}10^4$ cells/well. Plastic L, Synthemax II LC, Synthemax II HC, Collagen, PronectinF, FACT III and Cytodex I performed similarly between each other, yielding between $4.5\text{x}10^4$ and $6.4\text{x}10^4$ cells/well. Plastic Plus and Star-Plus microcarriers yielded low cell numbers, lower than $3.0\text{x}10^4$ cells/well. All microcarriers except Star-Plus led to increase cell number across the days of culture, where after day 3 there was an increase in cell number/well (Figure 2 A).

A second experiment was performed using ultra-low attachment 6-well plates using an increased working volume but maintaining scalable parameters. The number of microcarriers per well surface and the same initial seeding density of 6000 cells/cm^2 were used. Haemocytometer counts were performed to measure viable cell density on day 7 and phenotypic changes were assessed through RT-

qPCR. Plastic microcarriers led to the highest cell numbers ($1.7\pm0.1x10^6$ cells/mL), while Plastic Plus led to the lowest numbers ($7.5\pm0.4x10^5$ cells/mL) (Figure 3 A). Cell viability analysis revealed >95% viability of PA5 hOMCs on all microcarriers tested (Figure 3 B). Metabolite analysis of glucose, lactate and ammonium were performed on day 7 (Figure 3 C, D and E). Glucose concentrations were all between 4 - 8.5 mM, with Plastic showing the lower concentration and Plastic Plus the highest. The opposite trend was seen for lactate concentration with values between 12 - 16.5 mM. The concentration of ammonia was similar between all conditions with 0.8 mM for all microcarriers, except for Plastic microcarriers which produced a concentration of 0.65±0.1 mM. The phenotype of PA5 hOMCs was investigated using RT-qPCR. It is known that the olfactory mucosa population of cells harbours a mix of different cell types including mesenchymal stem cells, neural stem cells, fibroblasts and olfactory ensheathing cells (OECs). The OEC phenotype has been characterised by the expression of the glial markers $p75^{NTR}$, S100β, GFAP and the neural stem cell marker nestin and early neural differentiation marker β-III tubulin. Fibronectin has been used as a marker of 'contaminating' cell types as it can indicate the presence of fibroblasts. Results show the upregulation of neural stem cell markers β-III tubulin for Plastic L, Plastic and Plastic Plus microcarriers by 2-fold, and nestin for Plastic and Plastic Plus by 1.6-fold (Figure 3 F). Given the phenotypic traits obtained for cells grown in ultra-low attachment in 6 well-plates, with the objective to create a scalable bioprocess, Plastic and Plastic Plus were subsequently used to grow PA5 hOMCs in agitated cell culture conditions in spinner flasks.

Expansion of hOMCs in microcarriers suspension culture using spinner-flasks

PA5 hOMCs growth and metabolic profile in cell cultures using Plastic and Plastic Plus microcarriers

A method previously developed by Santos et al 2011 was adopted to performed PA5 hOMCs microcarrier cell culture in spinner flasks. A total working volume of 80 mL in 100-mL Belco spinner flasks was used with 50% of media change every two days, for a total of 7 days. An initial seeding density of 6000 cells/cm^2 was used, which is equivalent to $3.4x10^4$ cells/mL. Figure 4 A shows that both Plastic and Plastic Plus microcarrier cultures experienced a decrease in cell concentration after day 1 from $3.4\pm0.03x10^4$ cells/mL to $1.4\pm0.3x10^4$ cells/mL and $9.4\pm1.3x10^3$ cells/mL, respectively. Cell number started increasing after day 3. On day 7, the concentration of cells in cultures employing Plastic microcarriers was $1.4\pm1.1x10^5$ cells/mL and for Plastic Plus microcarriers was $4.9\pm1.8x10^4$ cells/mL (statistically significant, $p<0.05$). Cell viability remained above 90% (Figure 4 A) throughout the culture period. Representative images of Hoechst-counterstained PA5 hOMCs attached on Plastic and Plastic Plus microcarriers for each day of sample show cells were expanding on the microcarriers (Figure 4 E). Moreover, PA5 cells were completely detached from the microcarriers following the harvest in a gentle dissociation reagent and agitated conditions with high viability (Figure 4 F). Metabolic analysis of glucose, lactate and ammonia revealed similar concentration of these nutrient and metabolites for both conditions (Figure 4 B-D). On day 7, glucose concentration was of 10.5±1.7 mM and 11.5±1.6 mM, while lactate concentration was of 7.3±2.3 mM to 5.2±2.5 mM, for PA5 hOMCs grown on Plastic and Plastic Plus, respectively. The concentration of ammonia was of 0.7 mM for both conditions. Considering an exponential phase starting on day 3, specific consumption of glucose, specific production of lactate and ammonia, as well as yield of lactate per glucose were calculated. PA5 hOMCs grown of Plastic Plus led to a specific glucose consumption rate of 24.4±2.3 $pmol.day^{-1}cell^{-1}$,

similar to the one measure for PA5 hOMCs grown on Plastic which was 20.4±4.7 pmol.day^{-1}cell^{-1}. Specific production rates for lactate and ammonia was 47.9±6.3 pmol.day^{-1}cell^{-1} and 0.6±0.1 pmol.day^{-1}cell^{-1}, respectively for PA5 hOMCs grown on Plastic Plus. These results were on average 2 times higher than the specific production rates observed for PA5 hOMCs grown on Plastic microcarriers (24.6±7.2 pmol.day^{-1}cell^{-1} and 0.3±0.05 pmol.day^{-1}cell^{-1} for lactate and ammonia, respectively). The yield of lactate per glucose was 1.4±0.4 and 2.0±0.3 for PA5 hOMCs grown on Plastic and Plastic Plus microcarriers, respectively.

PA5 hOMCs phenotype and promotion of neuron outgrowth after growth on Plastic and Plastic Plus microcarrier suspension culture

Immunocytochemistry was performed for characteristic hOMCs biomarkers as presented in Figure 5 for PA5 hOMCs grown on Plastic and Plastic Plus microcarriers for 7 days. Immunocytochemistry results show the expression of p75^{NTR}, GFAP, S100β (glial markers), β-III tubulin, nestin (neural markers), fibronectin (fibroblastic marker) on both Plastic and Plastic Plus microcarriers. RT-qPCR results (Figure 6 A and B), show the upregulation of several markers for PA5 hOMCs grown on Plastic Plus compared to cells at day 0. β-III tubulin (2.3-fold), Fibronectin (3.5-fold), KDR (2.9-fold) and Sox9 (2.9-fold) are upregulated for PA5 hOMCs grown on Plastic Plus microcarriers compared to PA5 hOMCs grown on Plastic microcarriers by day 7. Most importantly, p75^{NTR}, a neurotrophic marker expressed by OECs is expressed 2.3-fold more on day 7 by PA5 hOMCs grown on Plastic Plus microcarriers compared with cells on day 0, while PA5 hOMCS grown on Plastic microcarriers maintained the same level of expression of this marker (1.0-fold) ($p<0.05$). Furthermore, a co-culture assay with NG108-15 cells was used as an assay indicative of the capacity of PA5 hOMCs to promote neurite outgrowth, using F7 Schwan cells as positive control and NG108-15 cell only as a negative control. Representative images used to quantify neurite outgrowth are shown in Figure 5 C. The average neurite length was 36±1.3 µm for Plastic Plus microcarriers, significantly higher ($p<0.05$) than the average neurite length obtained for Plastic (29.1±1.5 µm) microcarriers and the positive control (27.9±0.1 µm) (Figure 5 D). The maximum neurite length obtained for Plastic Plus was 96±7.0 µm, significantly higher ($p<0.05$) than the maximum neurite length obtained for Plastic microcarriers (81.8±3.2 µm) and the positive control (57.9±3.3 µm) (Figure 5 E). The average neurite per neuron was of 0.38±0.05, significantly higher ($p<0.05$) than the one obtained for cells grown on Plastic microcarriers (0.23±0.02) and the positive control (0.22±0.04) (Figure 5 F).

Discussion

PA5 hOMCs are a potential candidate therapy for an allogeneic cell therapy for the treatment of spinal cord injury (Santiago-Toledo et al., 2019). High cell doses of up to 1 billion cells will be required to produce cell banks to be supplied to patients (Casarosa et al., 2014). It has been shown that stirred tank bioreactor cell culture using microcarriers is a reliable, reproducible method to achieve high numbers of cells in a scalable manner (Qiu et al., 2016; Rafiq et al., 2013; Carlos AV Rodrigues et al., 2018; Santos et al., 2011). The first step to develop such a production method would be to select the right type of microcarrier and several authors have shown the successful screening of microcarriers for the growth of MSCs and NSCs (T. Chen et al., 2011; Rafiq et al., 2016; Carlos A. V. Rodrigues et al., 2011). Therefore, a similar strategy to those already presented for other cell types was used and in addition cell phenotype analysis was performed. PA5 hOMCs growth was followed for 7 days on

microcarriers using static 96-well plates. In terms of cell concentration after 7 days, while Plastic, Plastic L, Synthemax II LC, Synthemax II HC and PronectinF showed the most promising results, FACT III, Plastic Plus and Star-Plus microcarriers led to the lowest cell yields. Interestingly, it was observed that in spite of PA5 hOMCs efficiently attached to Plastic Plus microcarriers, the yield of cells on day 7 was lower than all other microcarriers with similar attachment efficiency (Plastic, Plastic L, Synthemax II LC, Synthemax II HC, and Collegen). This observation suggests that PA5 hOMCs grown on Plastic Plus microcarriers results in a slower growing population, in contrast with cells grown on neutrally charged surfaces. Interestingly, this has been reported for other anchorage-dependent cell types such as BM-MSCs (Rafiq et al., 2016).

In order to further investigate the phenotype of PA5 hOMCs after 7 days of culture, static microcarrier cultures on ultra-low attachment 96-well plates were scaled up to ultra-low 6-well plates. Interestingly, RT-qPCR results show the upregulation of neural stem cell marker nestin and early neural differentiation marker β-III tubulin on Plastic and Plastic Plus microcarriers. Neural stem cells are a cell type present in the olfactory mucosa (Delorme et al., 2010; Murrell et al., 2005; Nash et al., 2001) and may therefore be regenerative constituents of the PA5 hOMC populations. The upregulation of nestin for cells grown on Plastic and Plastic Plus microcarriers could contribute to increased neural regeneration, and may have led to the survival of olfactory neurons, displaying the expression of β-III tubulin, an early neural differentiation marker. Furthermore, even though Plastic Plus microcarriers did not led to such an increase in cell number, positive surfaces have been used in the past to promote attachment of neuronal cell types that may lead to neural regeneration (Kozak et al., 1978).

These results led to the selection of Plastic and Plastic Plus microcarriers for suspension culture in spinner flasks following a previously described method to grow hMSCs (Santos et al., 2011). Plastic L microcarriers were not taken into further studies due to the impracticality of in-house coating of microcarriers which is an additional expense and manipulation which would have to be considered in the manufacturing process.

Suspension microcarrier culture of PA5 hOMCs was carried out for 7 days. After day 1, a drop in viable cell concentration was observed due to only around 70-75% of cells attaching for both conditions, indicating inefficient cell attachment. After day 3, cells in both conditions start to grow, however, lower cell expansion was observed on Plastic Plus microcarriers. Thus Plastic microcarriers may encourage expansion of faster growing clones. By day 7 significantly higher viable cell concentration is obtained for PA5 hOMCs grown on Plastic microcarriers compared to Plastic Plus microcarriers, showing comparable results to studies performed in ultra-low attachment well-plates. Even though lower amount of PA5 hOMCs was obtained on Plastic Plus microcarriers on day 7, compared to Plastic microcarriers, cultures produced similar concentrations of glucose, lactate and ammonia over time. The concentrations of ammonium and lactate were below the reported inhibitory levels for hMSCs of 35.4 mM and 5.8 mM, respectively (Schop et al., 2009). Therefore, it is unlikely that the concentration of lactate and ammonia had a negative impact on PA5 hOMCs growth, assuming that hOMCs and hMSCs share similar metabolic response properties. The specific consumption of glucose was similar for both cultures, while the production of lactate and ammonia was double the amount for PA5 hOMCs grown on Plastic Plus microcarriers. In this study, the yield of lactate from

glucose is close to 2 for PA5 hOMCs grown in both conditions, suggesting that glucose is metabolised through aerobic glycolysis. In aerobic glycolysis, in the presence of oxygen, glucose metabolism is shifted from OXPHOS to glycolysis (Jones & Bianchi, 2015). These results can be explained by the upregulation of LDH activity promoted by the presence of the oncoprotein c-Myc (Shim et al., 1998). The PA5 hOMCs population is genetically modified with a fusion gene, c-MycER^{TAM}, activated by the synthetic estrogen-like agonist 4-hydrotamoxifen (Santiago-Toledo et al., 2019; Wall et al., 2016).

Phenotype analysis performed through immunocytochemistry showed that expression of hOMCs characteristic biomarkers such as p75^{NTR}, GFAP, S100β (glial markers), β-III tubulin, nestin (neural markers), fibronectin (fibroblastic marker) was maintained on both Plastic and Plastic Plus microcarriers after 7 days of expansion. Phenotype analysis was also assessed through RT-qPCR for PA5 hOMCs harvested at day 7 from Plastic and Plastic Plus microcarriers. Neurotrophin receptor p75^{NTR} expression has been attributed to the presence of OECs, a slow adherent cell type present in the olfactory mucosa, which has been reported to promote neural regeneration (Franceschini & Barnett, 1996; Pixley, 1992; Ramon-Cueto et al., 1993). Phenotypic analysis performed through RT-qPCR, revealed the upregulation of p75^{NTR} more than 2.5-fold for PA5 hOMCs grown on Plastic Plus microcarriers compared to Plastic microcarriers, after day 7. Factors related to microcarrier surface such as charge and stiffness may have led to an increase in the expression of p75^{NTR} for PA5 hOMCs grown on Plastic Plus microcarriers (Yang et al., 2017). The upregulation of β-III tubulin, although not statistically significant, might indicate the presence of a higher number of early neural differentiated cells or the promotion of survival of olfactory neurons on Plastic Plus microcarriers compared to Plastic microcarriers on day 7.

PA5 hOMCs potency was assessed in terms of ability to promote neurite outgrowth in a co-culture assay with NG108-15 cells. Results reveal that PA5 hOMCs grown on Plastic and Plastic Plus microcarriers retained promising functional activity. Studies of PNS repair which employed this assay shown that neurite outgrowth *in vitro* can be associated with Schwann cell potency to enhance neurite length *in vivo* (Daud et al., 2012; Jonsson et al., 2013).

The increased neurite outgrowth observed on NG108 co-culture assay using PA5 hOMCs grown on Plastic Plus microcarriers is likely to be related with the increased expression of p75^{NTR}, a marker of OECs (Delorme et al., 2010; J. R. Doucette, 1984; Lindsay et al., 2013; Wolozin et al., 1992). Therefore it is hypothesized that Plastic Plus led to an enrichment of OECs, which were then responsible for the increase in neurite outgrowth on this condition. In order to fully elucidate the mechanism of action it will be necessary to subclone the PA5 hOMCs population. These clones will have to be phenotypically characterized through immunocytochemistry or flow cytometry, expanded and checked for potency using the NG108 co-culture assay as well as animal studies.

In conclusion, we have demonstrated that expansion of PA5 hOMCs on Plastic and Plastic Plus microcarriers in suspension culture in agitated culture using spinner flasks is permissive. This study shows that expanding c-MycER^{TAM}-derived hOMCs on Plastic Plus microcarriers leads to cells with increased potency and increased expression of p75^{NTR}, a marker expressed by OECs. The work presented in this manuscript is a proof of concept that reveals competing effects of microcarriers on cell expansion versus functional attributes, showing that designing scalable bioprocesses should not only be

driven by cell yields, but also by phenotype and potency. This method contributes for the design of a bioprocess that in the future can support the expansion of clones of the PA5 hOMCs population in order to create an off-the-shelf advanced therapy for the treatment of CNS injuries such as those for the spinal cord.

Acknowledgements

This work was supported by grants from the National Council of Science and Technology of Mexico (CONACyT, Gerardo Santiago-Toledo), the Engineering and Physical Sciences Research Council (Gerardo Santiago-Toledo), and the Peter Dunnill Scholarship (Ana Valinhas).

Author Contribution Statement

Ana Valinhas and Gerardo Santiago-Toledo contributed equally.

References

Ahuja, C. S., Nori, S., Tetreault, L., Wilson, J., Kwon, B., Harrop, J., Choi, D., & Fehlings, M. G. (2017). Traumatic Spinal Cord Injury—Repair and Regeneration. *Neurosurgery*, *80*(3S), S9–S22. https://doi.org/10.1093/neuros/nyw080

Anna, Z., Katarzyna, J.-W., Joanna, C., Barczewska, M., Joanna, W., & Wojciech, M. (2017). Therapeutic Potential of Olfactory Ensheathing Cells and Mesenchymal Stem Cells in Spinal Cord Injuries. *Stem Cells International*, *2017*, 1–6. https://doi.org/10.1155/2017/3978595

Au, W. W., Treloar, H. B., & Greer, C. A. (2002). Sublaminar organization of the mouse olfactory bulb nerve layer. *The Journal of Comparative Neurology*, *446*(1), 68–80. http://www.ncbi.nlm.nih.gov/pubmed/11920721

Badenes, S. M., Fernandes, T. G., Miranda, C. C., Pusch-Klein, A., Haupt, S., Rodrigues, C. A., Diogo, M. M., Brüstle, O., & Cabral, J. M. (2017). Long-term expansion of human induced pluripotent stem cells in a microcarrier-based dynamic system. *Journal of Chemical Technology & Biotechnology*, *92*(3), 492–503. https://doi.org/10.1002/jctb.5074

Bianco, J. I., Perry, C., Harkin, D. G., Mackay-Sim, A., & Féron, F. (2004). Neurotrophin 3 promotes purification and proliferation of olfactory ensheathing cells from human nose. *Glia*, *45*(2), 111–123. https://doi.org/10.1002/glia.10298

Bickenbach, J., Office, A., Shakespeare, T., & von Groote, P. (2013). *International perspectives on spinal cord injury*. World Health Organization.

Brandenberger, R., Burger, S., Campbell, A., Lapinskas, E., & Rowley, J. A. (2011). Cell Therapy Bioprocessing. *BioProcess International*, *9*(3), S30–S37.

Casarosa, S., Bozzi, Y., & Conti, L. (2014). Neural stem cells: ready for therapeutic applications? *Molecular and Cellular Therapies*, *2*(1), 31. https://doi.org/10.1186/2052-8426-2-31

Chen, C., Kachramanoglou, C., Li, D., Andrews, P., & Choi, D. (2014). Anatomy and Cellular Constituents of the Human Olfactory Mucosa: A Review. *Journal of Neurological Surgery Part B: Skull Base*, *75*(05), 293–300. https://doi.org/10.1055/s-0033-1361837

Chen, T., Arslan, F., Yin, Y., Tan, S., Lai, R., Choo, A., Padmanabhan, J., Lee, C., de Kleijn, D. P., & Lim, S. (2011). Enabling a robust scalable manufacturing process for therapeutic exosomes through oncogenic immortalization of human ESC-derived MSCs. *Journal of Translational Medicine*, *9*(1), 47. https://doi.org/10.1186/1479-5876-9-47

Daud, M. F. B., Pawar, K. C., Claeyssens, F., Ryan, A. J., & Haycock, J. W. (2012). An aligned 3D neuronal-glial co-culture model for peripheral nerve studies. *Biomaterials*, *33*(25), 5901–5913. https://doi.org/10.1016/j.biomaterials.2012.05.008

Delorme, B., Nivet, E., Gaillard, J., Häupl, T., Ringe, J., Devèze, A., Magnan, J., Sohier, J., Khrestchatisky, M., Roman, F. S., Charbord, P., Sensebé, L., Layrolle, P., & Féron, F. (2010). The Human Nose Harbors a Niche of Olfactory Ectomesenchymal Stem Cells Displaying Neurogenic and Osteogenic Properties. *Stem Cells and Development*, *19*(6), 853–866. https://doi.org/10.1089/scd.2009.0267

dos Santos, F., Campbell, A., Fernandes-Platzgummer, A., Andrade, P. Z., Gimble, J. M., Wen, Y., Boucher, S., Vemuri, M. C., da Silva, C. L., & Cabral, J. M. S. (2014). A xenogeneic-free bioreactor system for the clinical-scale expansion of human mesenchymal stem/stromal cells. *Biotechnology and Bioengineering*, *111*(6), 1116–1127. https://doi.org/10.1002/bit.25187

Doucette, J. R. (1984). The glial cells in the nerve fiber layer of the rat olfactory bulb. *The Anatomical Record*, *210*(2), 385–391. https://doi.org/10.1002/ar.1092100214

Doucette, R. (1991). PNS-CNS transitional zone of the first cranial nerve. *The Journal of Comparative Neurology*, *312*(3), 451–466. https://doi.org/10.1002/cne.903120311

Féron, F., Perry, C., Cochrane, J., Licina, P., Nowitzke, A., Urquhart, S., Geraghty, T., & Mackay-Sim,

A. (2005). Autologous olfactory ensheathing cell transplantation in human spinal cord injury. *Brain*, *128*(12), 2951–2960. https://doi.org/10.1093/brain/awh657

Féron, F, Mackay-Sim, A., Andrieu, J.., Matthaei, K.., Holley, A., & Sicard, G. (1999). Stress induces neurogenesis in non-neuronal cell cultures of adult olfactory epithelium. *Neuroscience*, *88*(2), 571–583. https://doi.org/10.1016/S0306-4522(98)00233-4

Féron, François, Perry, C., McGrath, J. J., & Mackay-Sim, A. (1998). New Techniques for Biopsy and Culture of Human Olfactory Epithelial Neurons. *Archives of Otolaryngology–Head & Neck Surgery*, *124*(8), 861. https://doi.org/10.1001/archotol.124.8.861

Franceschini, I. A., & Barnett, S. C. (1996). Low-Affinity NGF-Receptor and E-N-CAM Expression Define Two Types of Olfactory Nerve Ensheathing Cells That Share a Common Lineage. *Developmental Biology*, *173*(1), 327–343. https://doi.org/10.1006/dbio.1996.0027

Gómez-Virgilio, L., Ramírez-Rodríguez, G. B., Sánchez-Torres, C., Ortiz-López, L., & Meraz-Ríos, M. A. (2018). Soluble Factors from Human Olfactory Neural Stem/Progenitor Cells Influence the Fate Decisions of Hippocampal Neural Precursor Cells. *Molecular Neurobiology*. https://doi.org/10.1007/s12035-018-0906-2

Hahn, C.-G., Han, L.-Y., Rawson, N. E., Mirza, N., Borgmann-Winter, K., Lenox, R. H., & Arnold, S. E. (2005). In vivo and in vitro neurogenesis in human olfactory epithelium. *The Journal of Comparative Neurology*, *483*(2), 154–163. https://doi.org/10.1002/cne.20424

Holbrook, E. H., Wu, E., Curry, W. T., Lin, D. T., & Schwob, J. E. (2011). Immunohistochemical characterization of human olfactory tissue. *The Laryngoscope*, *121*(8), 1687–1701. https://doi.org/10.1002/lary.21856

Ito, D., Ibanez, C., Ogawa, H., Franklin, R. J. M., & Jeffery, N. D. (2006). Comparison of cell populations derived from canine olfactory bulb and olfactory mucosal cultures. *American Journal of Veterinary Research*, *67*(6), 1050–1056. https://doi.org/10.2460/ajvr.67.6.1050

Iwatsuki, K., Yoshimine, T., Kishima, H., Aoki, M., Yoshimura, K., Ishihara, M., Ohnishi, Y., & Lima, C. (2008). Transplantation of olfactory mucosa following spinal cord injury promotes recovery in rats. *NeuroReport*, *19*(13), 1249–1252. https://doi.org/10.1097/WNR.0b013e328305b70b

Jani, H. R., & Raisman, G. (2004). Ensheathing cell cultures from the olfactory bulb and mucosa. *Glia*, *47*(2), 130–137. https://doi.org/10.1002/glia.20038

Jones, W., & Bianchi, K. (2015). Aerobic Glycolysis: Beyond Proliferation. *Frontiers in Immunology*, *6*. https://doi.org/10.3389/fimmu.2015.00227

Jonsson, S., Wiberg, R., McGrath, A. M., Novikov, L. N., Wiberg, M., Novikova, L. N., & Kingham, P. J. (2013). Effect of Delayed Peripheral Nerve Repair on Nerve Regeneration, Schwann Cell Function and Target Muscle Recovery. *PLoS ONE*, *8*(2), e56484. https://doi.org/10.1371/journal.pone.0056484

Kawaja, M. D., Boyd, J. G., Smithson, L. J., Jahed, A., & Doucette, R. (2009). Technical Strategies to Isolate Olfactory Ensheathing Cells for Intraspinal Implantation. *Journal of Neurotrauma*, *26*(2), 155–177. https://doi.org/10.1089/neu.2008.0709

Kozak, L. P., Eppig, J. J., Dahl, D., & Bignami, A. (1978). Enhanced neuronal expression in reaggregating cells of mouse cerebellum cultured in the presence of poly-l-lysine. *Developmental Biology*, *64*(2), 252–264. https://doi.org/10.1016/0012-1606(78)90076-3

Lindsay, S. L., Johnstone, S. A., Mountford, J. C., Sheikh, S., Allan, D. B., Clark, L., & Barnett, S. C. (2013). Human mesenchymal stem cells isolated from olfactory biopsies but not bone enhance CNS myelination in vitro. *Glia*, *61*(3), 368–382. https://doi.org/10.1002/glia.22440

Mackay-Sim, A., Feron, F., Cochrane, J., Bassingthwaighte, L., Bayliss, C., Davies, W., Fronek, P., Gray, C., Kerr, G., Licina, P., Nowitzke, A., Perry, C., Silburn, P. A. S., Urquhart, S., & Geraghty, T. (2008). Autologous olfactory ensheathing cell transplantation in human paraplegia: a 3-year clinical trial. *Brain*, *131*(9), 2376–2386. https://doi.org/10.1093/brain/awn173

Meijering, E., Jacob, M., Sarria, J.-C. F., Steiner, P., Hirling, H., & Unser, M. (2004). Design and validation of a tool for neurite tracing and analysis in fluorescence microscopy images. *Cytometry*, *58A*(2), 167–176. https://doi.org/10.1002/cyto.a.20022

Murrell, W., Féron, F., Wetzig, A., Cameron, N., Splatt, K., Bellette, B., Bianco, J., Perry, C., Lee, G., & Mackay-Sim, A. (2005). Multipotent stem cells from adult olfactory mucosa. *Developmental Dynamics*, *233*(2), 496–515. https://doi.org/10.1002/dvdy.20360

Nash, H. H., Borke, R. C., & Anders, J. J. (2001). New method of purification for establishing primary cultures of ensheathing cells from the adult olfactory bulb. *Glia*, *34*(2), 81–87. https://doi.org/10.1002/glia.1043

Oh, S. K. W., Chen, A. K., Mok, Y., Chen, X., Lim, U.-M., Chin, A., Choo, A. B. H., & Reuveny, S. (2009). Long-term microcarrier suspension cultures of human embryonic stem cells. *Stem Cell Research*, *2*(3), 219–230. https://doi.org/10.1016/j.scr.2009.02.005

Pixley, S. K. (1992). The olfactory nerve contains two populations of glia, identified both in vivo and in vitro. *Glia*, *5*(4), 269–284. https://doi.org/10.1002/glia.440050405

Qiu, L., Lim, Y. M., Chen, A. K., Reuveny, S., Oh, S. K. W., Tan, E. K., & Zeng, L. (2016). Microcarrier-Expanded Neural Progenitor Cells Can Survive, Differentiate, and Innervate Host Neurons Better When Transplanted as Aggregates. *Cell Transplantation*, *25*(7), 1343–1357. https://doi.org/10.3727/096368915X690378

Rafiq, Q. A., Brosnan, K. M., Coopman, K., Nienow, A. W., & Hewitt, C. J. (2013). Culture of human mesenchymal stem cells on microcarriers in a 5 l stirred-tank bioreactor. *Biotechnology Letters*, *35*(8), 1233–1245. https://doi.org/10.1007/s10529-013-1211-9

Rafiq, Q. A., Coopman, K., Nienow, A. W., & Hewitt, C. J. (2016). Systematic microcarrier screening and agitated culture conditions improves human mesenchymal stem cell yield in bioreactors. *Biotechnology Journal*, *11*(4), 473–486. https://doi.org/10.1002/biot.201400862

Ramon-Cueto, A., Perez, J., & Nieto-Sampedro, M. (1993). In vitro enfolding of olfactory neurites by p75 NGF receptor positive ensheathing cells from adult rat olfactory bulb. *Eur J Neurosci*, *5*(9), 1172–1180.

Reshamwala, R., Shah, M., St John, J., & Ekberg, J. (2019). Survival and Integration of Transplanted Olfactory Ensheathing Cells are Crucial for Spinal Cord Injury Repair: Insights from the Last 10 Years of Animal Model Studies. *Cell Transplantation*, *28*(1_suppl), 132S-159S. https://doi.org/10.1177/0963689719883823

Rodrigues, Carlos AV, Silva, T. P., Nogueira, D. E., Fernandes, T. G., Hashimura, Y., Wesselschmidt, R., Diogo, M. M., Lee, B., & Cabral, J. M. (2018). Scalable culture of human induced pluripotent cells on microcarriers under xeno-free conditions using single-use vertical-wheel™ bioreactors. *Journal of Chemical Technology & Biotechnology*. https://doi.org/10.1002/jctb.5738

Rodrigues, Carlos A. V., Diogo, M. M., da Silva, C. L., & Cabral, J. M. S. (2011). Microcarrier expansion of mouse embryonic stem cell-derived neural stem cells in stirred bioreactors. *Biotechnology and Applied Biochemistry*, *58*(4), 231–242. https://doi.org/10.1002/bab.37

Santiago-Toledo, G., Georgiou, M., dos Reis, J., Roberton, V. H., Valinhas, A., Wood, R. C., Phillips, J. B., Mason, C., Li, D., Li, Y., Sinden, J. D., Choi, D., Jat, P. S., & Wall, I. B. (2019). Generation of c-MycERTAM-transduced human late-adherent olfactory mucosa cells for potential regenerative applications. *Scientific Reports*, *9*(1), 1–13. https://doi.org/10.1038/s41598-019-49315-6

Santos, F. dos, Andrade, P. Z., Abecasis, M. M., Gimble, J. M., Chase, L. G., Campbell, A. M., Boucher, S., Vemuri, M. C., Silva, C. L. da, & Cabral, J. M. S. (2011). Toward a Clinical-Grade Expansion of Mesenchymal Stem Cells from Human Sources: A Microcarrier-Based Culture System Under Xeno-Free Conditions. *Tissue Engineering Part C: Methods*, *17*(12), 1201–1210. https://doi.org/10.1089/ten.tec.2011.0255

Schop, D., Janssen, F. W., van Rijn, L. D. S., Fernandes, H., Bloem, R. M., de Bruijn, J. D., & van Dijkhuizen-Radersma, R. (2009). Growth, Metabolism, and Growth Inhibitors of Mesenchymal Stem Cells. *Tissue Engineering Part A*, *15*(8), 1877–1886. https://doi.org/10.1089/ten.tea.2008.0345

Shim, H., Chun, Y. S., Lewis, B. C., & Dang, C. V. (1998). A unique glucose-dependent apoptotic pathway induced by c-Myc. *Proceedings of the National Academy of Sciences*, *95*(4), 1511–1516. https://doi.org/10.1073/pnas.95.4.1511

Simaria, A. S., Hassan, S., Varadaraju, H., Rowley, J., Warren, K., Vanek, P., & Farid, S. S. (2014). Allogeneic cell therapy bioprocess economics and optimization: Single-use cell expansion technologies. *Biotechnology and Bioengineering*, *111*(1), 69–83. https://doi.org/10.1002/bit.25008

Tabakow, P., Jarmundowicz, W., Czapiga, B., Fortuna, W., Miedzybrodzki, R., Czyz, M., Huber, J., Szarek, D., Okurowski, S., Szewczyk, P., Gorski, A., & Raisman, G. (2013). Transplantation of Autologous Olfactory Ensheathing Cells in Complete Human Spinal Cord Injury. *Cell Transplantation*, *22*(9), 1591–1612. https://doi.org/10.3727/096368912X663532

Wall, I. B., Santiago Toledo, G., & Jat, P. S. (2016). Recent advances in conditional cell immortalization technology. *Cell and Gene Therapy Insights*, *2*(3), 391–396. https://doi.org/10.18609/cgti.2016.041

Wolozin, B., Sunderland, T., Zheng, B., Resau, J., Dufy, B., Barker, J., Swerdlow, R., & Coon, H. (1992). Continuous culture of neuronal cells from adult human olfactory epithelium. *Journal of Molecular Neuroscience*, *3*(3), 137–146. https://doi.org/10.1007/BF02919405

Yang, Y., Wang, K., Gu, X., & Leong, K. W. (2017). Biophysical Regulation of Cell Behavior—Cross Talk between Substrate Stiffness and Nanotopography. *Engineering*, *3*(1), 36–54. https://doi.org/10.1016/J.ENG.2017.01.014

Yiu, G., & He, Z. (2006). Glial inhibition of CNS axon regeneration. *Nature Reviews Neuroscience*, *7*(8), 617–627. https://doi.org/10.1038/nrn1956

Tables

Table 1 - List of microcarriers used and respective properties.

Microcarrier	Manufacturer	Diameter (µm)	Matrix	Surface coating/charge	Average density
Plastic	Pall	125-212	Polystyrene	None	1.02
Plastic Laminin coated (Plastic L)	Pall	125-212	Polystyrene	Cultrex ® Mouse Laminin I	1.02
Plastic Plus	Pall	125-212	Polystyrene	Cationic surface	1.02
PronectinF ®	Pall	125-212	Polystyrene	Recombinant Fibronectin	1.02
Collagen	Pall	125-212	Polystyrene	Type I porcine collagen	1.02
FACT III	Pall	125-212	Polystyrene	Type I porcine collagen	1.02
Star-Plus	Pall	125-212	Polystyrene	Cross-linked polystyrene	1.02
Hillex II	Pall	160-200	Polystyrene	Cross-linked polystyrene Cationic surface	1.09
Synthemax II ® (Low and High Concentration)	Corning	125-212	Polystyrene	Synthemax II ®	1.02
Cytodex I™	GE Healthcare	60-87	Dextran	Positively charged N,N-diethylaminoethyl groups	1.03

Table 2 - List of antibodies used for immunocytochemistry.

Reactivity	Antibody	Host	Company	Code
$p75^{NTR}$	IgG polyclonal	Rabbit	Millipore	ab1554
Fibronectin	IgG monoclonal	Mouse	Sigma	F6140
Nestin	IgG monoclonal	Mouse	Millipore	MAB5326
S100β	IgG polyclonal	Rabbit	Dako	Z0311
GFAP	IgG polyclonal	Rabbit	Dako	Z0334
β III Tubulin	IgG monoclonal	Mouse	Sigma	T8660
CD90	IgG monoclonal	Mouse	Millipore	MAB1406

Rabbit IgG (H+L)	IgG DyLight 594	Goat	Thermo Scientific	35560
Mouse IgG (H+L)	IgG DyLight 488	Goat	Thermo Scientific	35510

Table 3 - List of Primers used for qRT-PCR.

Biomarker	**Description**	**NCBI Accession**	**QuantiTect Primer Assay**	**Catalog Number**
$p75^{NTR}$	Glial Marker	NM_002507	Hs_NFGR_1_SG	QT00056756
S100β	Glial Marker	NM_006272	Hs_S100B_1_SG	QT00059164
GFAP	Glial Marker	NM_001131019	Hs_GFAP_1_SG	QT00081151
Nestin	Neural stem cell marker	NM_006617	Hs_NES_1SG	QT00235781
β-III-tubulin	Neural differentiation marker	NM_006086	Hs_TUBB3_vb.1_SG	QT02399950
Fibronectin	Cell adhesion marker	NM_002026	Hs_FN1_1_SG	QT00038024
CD34	Negative MSC Marker	NM_001773	Hs_CD34_1_SG	QT00998284
CD45	Negative MSC Marker	NM_002838	Hs_PTPRC_1_SG	QT00028791
CD73	MSC Marker	NM_002526	Hs_NT5E_1_SG	QT00027279
CD90	MSC Marker	NM_001311160	Hs_THY1_1_SG	QT00023569
CD105	MSC Marker	NM_00118	Hs_ENG_1SG	QT00013335
KDR	Endothelial Cell Marker	NM_002253	Hs_KDR_1_SG	QT00069818
Sox9	Chrondrogenic Marker	NM_000346	Hs_SOX9_1_SG	QT00001498
Runx2	Osteogenic Marker	NM_001015051	Hs_RUNX2_1_SG	QT00020517
SPP1	Osteogenic Marker	NM_000582	Hs_SPP1_1_SG	QT01008798
PPARγ	Adipogenic Marker	NM_005037	Hs_PPARG_1_SG	QT00029841
β-actin	Housekeeping gene	NM_001101	Hs_ACTB_2_SG	QT01680476

Figure Legends

Figure 1 - Growth and phenotype of PA5 hOMCs on monolayer culture. (A) Cell growth was quantified using the CCK-8 viability reagent for 7 days. (B) Brightfield image of cells in culture. Cells stained positive for (C) p75NTR, (D) S100β, (E) GFAP, (F) β-III tubulin, (G) nestin, (H) fibronectin, and CD90 (I). Cell nuclei were counterstained with Hoechst (blue). Data is represented as mean±SEM, n = 3. (Scale bar =400µm).

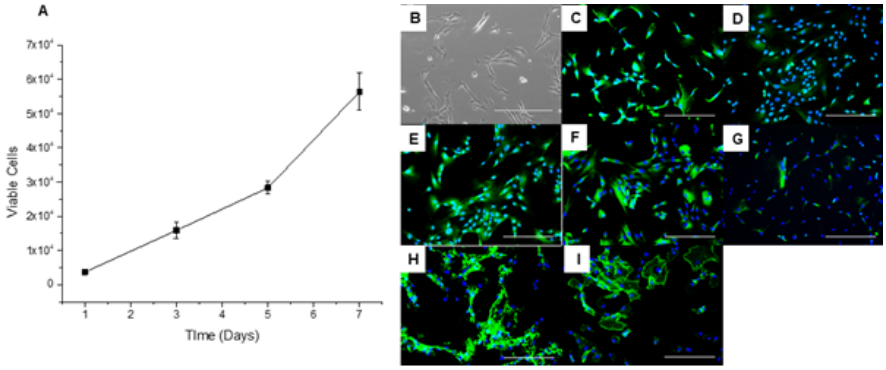

Figure 2 - PA5 hOMCs were grown on microcarriers in 96-well plates for 7 days on 10 different microcarriers. (A) Growth curve showing viable cells/well obtained through measurements of metabolite activity using the CCK-8 viability reagent. (B) Total viable cell/well achieved for each microcarrier on day 1. (C) Total viable cell/well achieved for each microcarrier on day 7. Data represented as mean ± SEM, n=3. Three independent repeats were performed for each condition. Significant differences were noted with (*) for $p<0.05$.

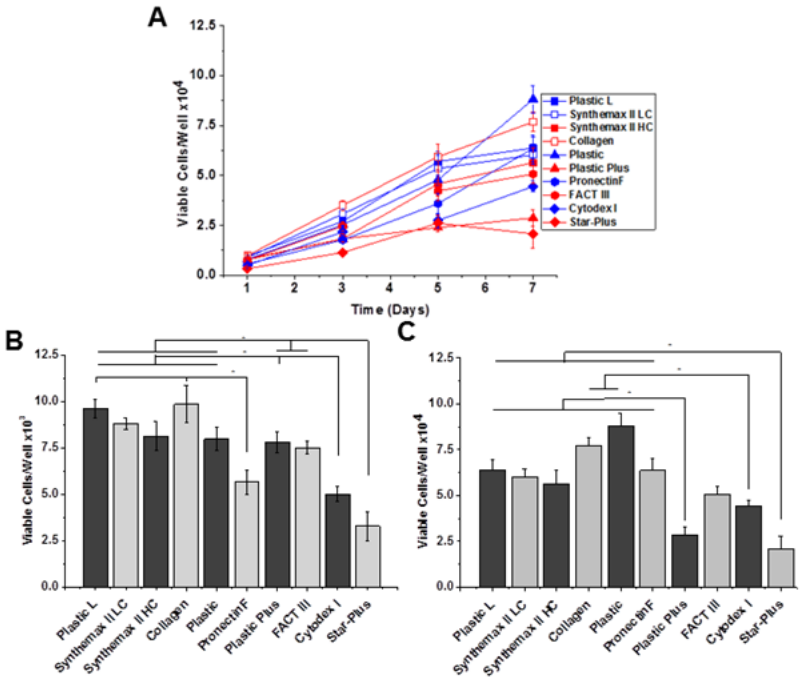

Figure 3– PA5 hOMCs were grown on Plastic L, Synthemax II LC, Collagen, Plastic, PronectinF and Plastic Plus microcarriers for 7 days with 50% media change every 2 days and using an initial seeding density of 6000 cells/cm^2. Viable cell concentration (A) and cell viability (B) were measured. Metabolite analysis for glucose (C), lactate (D), and ammonium (E) were performed. (F) Expression of p75^{NTR}, S100β, GFAP, β-III tubulin, nestin and fibronectin by PA5 hOMCs grown on Plastic L, Synthemax II LC, Collagen, Plastic, PronectinF and Plastic Plus, assessed through RT-qPCR on day 7. PA5 hOMCs before seeding were used as a reference. Data represented as mean ± SEM, n = 3. Three independent repeats were performed for each condition. Significant differences were noted with (*) for $p<0.05$.

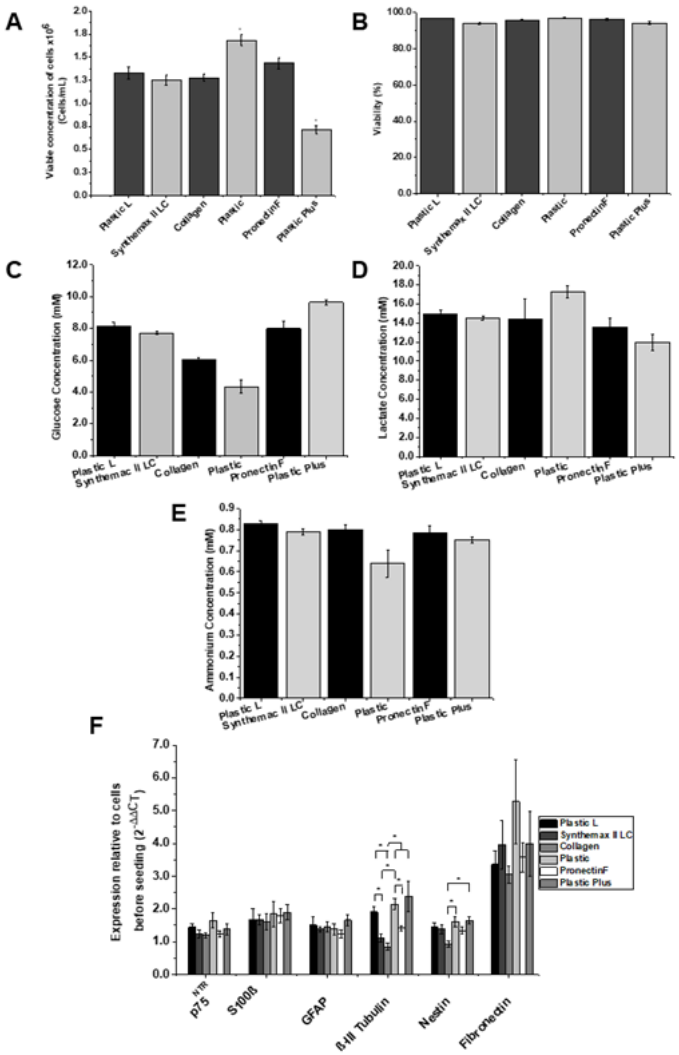

Figure 4- Comparison of PA5 hOMCs growth on Plastic and Plastic Plus microcarriers, in spinner flasks for 7 days. (A) Viable cell concentration (cells/mL) and cell viability was measured via haemocytometer counts. Metabolite analysis was performed to determine concentration of (B) glucose (mM), (C) lactate (mM) and (D) ammonium (mM). (E) Representative images of cells on Plastic and Plastic Plus microcarriers, for each day of sample. Hoechst was used as a nucleic dye. (F) Representative bright field pictures of PA5 cells before and after harvest from Plastic and Plastic Plus microcarriers. Data is presented as mean ± SEM, n=3. Three independent runs were performed for each spinner flask condition. Significant differences were noted with (*) for $p<0.05$. Scale bar = 200 µm.

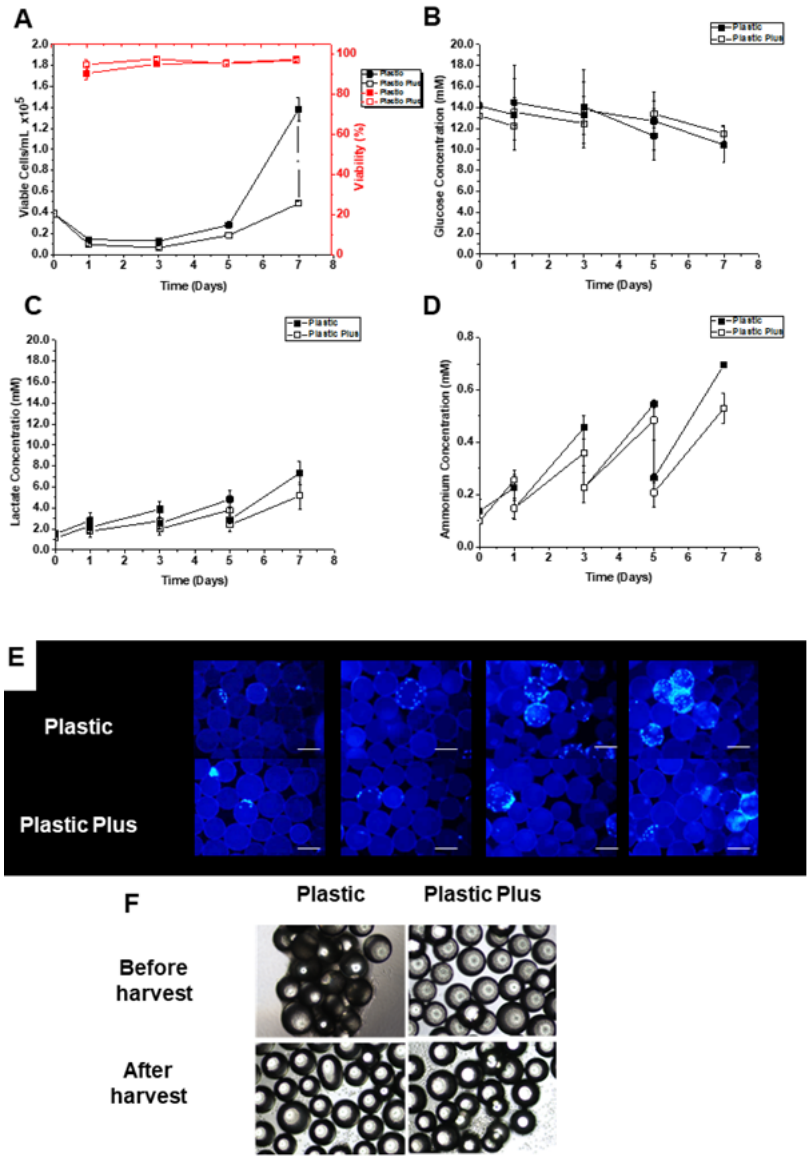

Figure 5 – Expression of $p75^{NTR}$, GFAP, S100β (glial markers), β-III tubulin, nestin (neural markers), fibronectin (fibroblastic marker) after 7 days of growth of PA5 hOMCs on Plastic, Plastic Plus microcarriers under stirred suspension cultures in spinner flasks.

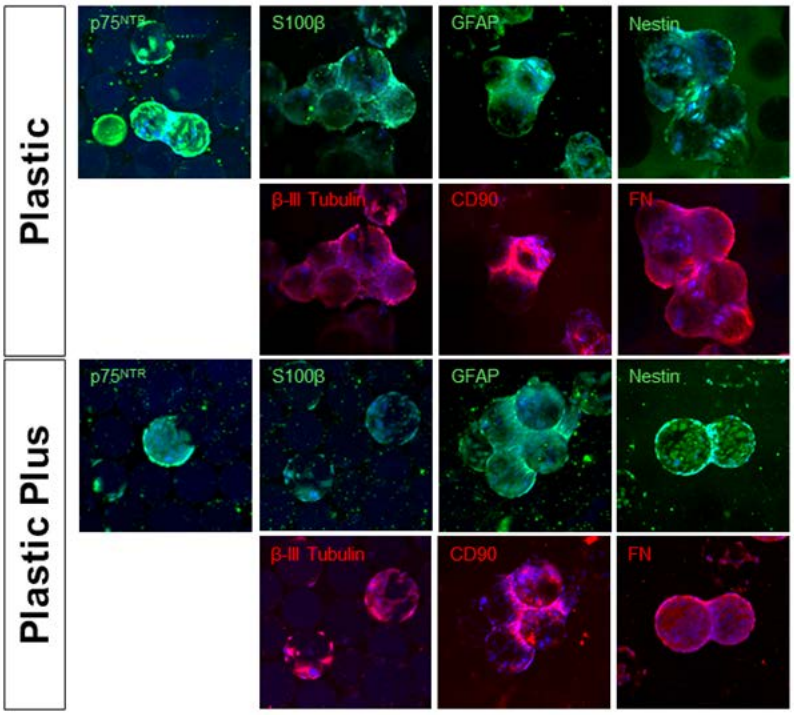

Figure 6 - The expression of $p75^{NTR}$, GFAP, S100β (glial markers), β-III tubulin, nestin (neural markers), fibronectin (fibroblastic marker), CD90, CD105, CD73 (positive MSCs markers), CD34, CD45 (negative MSCs markers), PPARg (adipogenesis marker), SPP1, Runx2 (osteogenesis markers), Sox9 (chondrogenesis marker) and VEGFR2 (endothelial cell marker). (A) Heat map for gene expression variation relative to cells before seeding. (B) Values of expression relative to cells before seeding. NG108-15 co-culture assay to assess the potential for neural regeneration of PA5 hOMCs. F7 Schwann cells were used as a positive control, and NG108-15 neurons only were used as negative control. (C) Representative images used to quantify neurite outgrowth. (D) Average neurite length, (E) maximum neurite length (F) average neurite per neuron, were higher for Plastic and especially Plastic Plus microcarriers (scale bar=400 µm). Data represented as mean ± SEM (n=3). Three independent runs were performed for each spinner flask condition. Significant differences were noted with (*) for $p<0.05$.